Temperature/pH dual sensitive *Hericium erinaceus* residue carboxymethyl chitin/poly (*N*-isopropyl acrylamide) sequential IPN hydrogels

Jing Liao · Huihua Huang

Abstract In this study, a novel temperature/pH dual responsive hydrogel, based on *Hericium erinaceus* residue carboxymethyl chitin (HCMC) and poly (*N*-isopropylacrylamide) (PNIPAm), was synthesized by sequential IPN technique. Series of IPN hydrogels were obtained by varying initial *N*-isopropylacrylamide (NIPAm) concentrations. The structure, morphology, thermal property, transparency, mechanical property, swelling kinetics, temperature/pH responses and 5-Fu release behavior of the prepared hydrogels were systematically investigated. The structure analysis results showed that the IPN hydrogels were successfully synthesized. The prepared hydrogels showed more compact network structure and enhanced mechanical property as NIPAm concentration increased, but reduced transparency, swelling degree and 5-Fu release ratio. More importantly, HCMC and PNIPAm ensured the pH and temperature responses, respectively. 5-Fu could be gradually released from the prepared hydrogels, which followed Fickian diffusion model. Therefore, the prepared hydrogels may be served as promising materials for drug delivery systems.

Introduction

Chitin, as one of the most abundant biopolymers in nature, is widely distributed in natural resources such as crustacean shells (crab, shrimp, prawn, lobster), mollusks (krill, oyster, clam shells, squid skeleton), various insects (cockroaches, silkworms, spiders, beetles) and fungi (mushrooms, yeast) (Croisier and Jérôme 2013). But commercial chitin is almost derived from crustacean shells, which limited its applications in some specific aspects (Liao and Huang 2019a). For instance, crustacean shells derived chitin materials could increase the risks of allergy. Hence exploitation of new chitin products from non-animal resources has been the major issue to broaden its applications. Mushroom, as the most typical non-animal resource of chitin, has been increasingly used to produce chitin (Bilbao-Sainz et al. 2017; Chien et al. 2016; Wu et al. 2004; Yen and Mau 2007). Compared with crustacean shells derived chitin, fungal chitin is easily obtained because mushroom is cultured without specific

J. Liao · H. Huang (✉)
School of Food Science and Engineering, South China University of Technology, Guangzhou 510641, China
e-mail: fehhuang@scut.edu.cn

geographic restrictions and could avoid allergic responses (Munoz et al. 2015). Therefore, mushroom could become an alternative non-animal resource of chitin, and mushroom industry residues should be utilized to produce chitin, because it is resource-saving and eco-friendly. *Hericium erinaceus* (HE) is a typical mushroom in China with total production of over 100 thousand tons each year. However, the exploitation of HE is mainly focused on *Hericium erinaceus* polysaccharides (HEPs), *Hericium erinaceus* residue (HER) was discarded with no suitable use. Therefore, the multipurpose utilization of HER is important, especially in the use of HER chitin, which is a desirable biopolymer for hydrogels preparation.

Hydrogels are physically or chemically cross-linked 3D hydrophilic polymeric networks, which could adsorb a lot of water without dissolution (Guo et al. 2015). Generally, hydrogels can be divided into smart and non-smart hydrogels. In particular, the smart hydrogels are increasingly concerned because of their ability to respond intelligently to changes in external environmental stimuli such as temperature (Sun et al. 2019), pH (Dai et al. 2019a), salt (Dai et al. 2019a), electric (Dai et al. 2018) and magnetic field (Dai et al. 2019b). These specific properties made smart hydrogels widely applied to drug delivery (Liu and Huang 2016), dye adsorption (Dai et al. 2018b) and enzyme immobilization (Dai et al. 2017; Liu et al. 2017a, b). Temperature and pH sensitive hydrogels are commonly studied because these properties can be easily controlled (Haq et al. 2017). However, native chitin hydrogels are lack of such response characteristics, the modification of chitin is needed.

Carboxymethylation of polysaccharide is a common functional modification to prepare bio-based materials with intelligent properties (Sun et al. 2019). Some polysaccharides such as chitosan, cellulose and xylan have been modified into carboxymethyl polymers for preparing smart biopolymer hydrogels (Azarova et al. 2016; Dai et al. 2018a, 2019a; Sun et al. 2019). Therefore, carboxymethyl chitin (CMC) can be used to prepare pH-sensitive hydrogels due to the presence of carboxyl groups.

Poly *N*-isopropylacrylamide (PNIPAm) is widely studied due to its lower critical solution temperature (LCST), which is close to human body temperature. PNIPAm hydrogels will undergo a reversible hydrophilic–hydrophobic phase transition around the LCST in aqueous system. When environmental temperature

is below LCST, PNIPAm hydrogels will be highly swollen. On the contrary, PNIPAm hydrogel will collapse and expel the contained water when external temperature is above LCST (Lima et al. 2012; Zhuo and Li 2003).

In order to achieve temperature/pH dual sensitivity, the combination of these two polymers is necessary. Compared with blending, IPN technique is more advocated because IPN hydrogels are more stable than the single crosslinking network (Pan et al. 2018). Usually, IPN hydrogels combined distinct coexisting network and could be divided into semi- or full IPN hydrogels. For semi-IPN hydrogels, although they contained differentiable coexisting network, one of the polymeric component is cross-linked in its own network, the other is just physically entrapped therein. The full IPN hydrogels are that all contained coexisting networks are cross-linked in their respective network (Roland 2013).

Until now, many efforts have been made for preparing hydrogels based on CMC and PNIPAm. Chen and Cheng (2006) prepared a thermo-responsive hydrogel by grafting PNIPAm onto chitosan through amide bond linkages. Wei et al. (2013) synthesized a carboxymethyl chitosan/polyacrylamide hydrogel by copolymerization, the prepared hydrogels showed pH and temperature sensitivity. Zhang et al. (2014) prepared a hydrogel with pH and thermal responses based on carboxymethyl chitosan, *N*-isopropyl acrylamide and glycidyl methacrylate by UV crosslinking. However, there is still lack of studies concerning combination of these two polymers by IPN technique.

As mentioned above, HCMC was synthesized homogeneously in NaOH/Urea solution based on the chitin extracted from HER, the synthesized HCMC was then cross-linked to form the first layer network, which was further used as the reaction matrix to in situ polymerization of NIPAm to form the second layer network. A series of HCMC/PNIPAm IPN hydrogels were prepared by varying the concentration of monomer (NIPAm). Temperature/pH dual sensitive behaviors should be produced due to the presence of HCMC and PNIPAm. The influence of NIPAm concentration on the structure, morphology, thermal stability, transparency, mechanical property, swelling kinetics and 5-Fu release performances of the prepared hydrogels was investigated.

Materials and methods

Materials and reagents

Chitin from *Hericium erinaceus* residue was obtained according to our previous study (Liao and Huang 2019b). The degree of acetylation (DA) and molecular weight (M_w) were determined to be 51.83% and 1.56×10^5 g/mol according to element analysis and viscosity method, respectively. Sodium monochloroacetate, *N*-isopropylacrylamide (NIPAm), *N*, *N'*-methylene bisacrylamide (MBA), ammonium persulfate (APS) was supplied by Aladdin Reagent Co. Ltd. (Shanghai city, China). Hydrogen chloride (36%, v/v), sodium hypochlorite, sodium hydroxide, urea, epichlorohydrin (ECH) were purchased from Guangzhou Chemical Reagent Co., Ltd. (Guangzhou city, Guangdong province, China). All chemicals were used without further purification and solutions were prepared by distilled water.

Hydrogels preparation

Scheme 1 displays the synthetic scheme of HCMC/PNIPAm sequential IPN hydrogels. Firstly, the preparation of HCMC was carried out by homogenous carboxymethylation of chitin in NaOH/urea solution according to Liu et al. (2016) with some modifications. In brief, 7% (m/v) chitin solution was prepared by dissolving HER chitin in NaOH/urea (11%/4%) solution by repeated freezing–thawing, followed by adding 70% (m/v) sodium monochloroacetate solution to the chitin solution at ratio of 1/10 under stirring at 0 °C for 30 min. Then the whole reaction was maintained at room temperature for 24 h. After that, ECH was gradually dropped into the resulted solutions at ratio of 1/10 under stirring at 0 °C for 30 min to obtain homogeneous solution. Finally, the resultant mixture was carefully poured into mold and kept at 60 °C for 2 h for complete crosslinking. After immersing in distilled water until neutral, HCMC hydrogels were available.

To synthesize second layer network inside HCMC hydrogels, the obtained HCMC hydrogels were firstly immersed in aqueous solution with certain concentrations of NIPAm (0%, 1%, 2% and 3%), MBA (0.5%) and APS (0.5%) for 12 h at room temperature. Then the second network was synthesized at 40 °C for another 12 h under N_2 atmosphere. The obtained hydrogels were washed with deionized water and named as IPN0, IPN1, IPN2 and IPN3 according to the concentration of NIPAm, respectively.

Characterization of the prepared hydrogels

The structures of the prepared hydrogels were investigated by ATR-FTIR (Vector 33, Bruker, Germany) and XRD (D8 ADVANCE, Bruker, Germany). The internal morphology of the prepared hydrogels was observed by a scanning electron microscope (S-3400 N, Hitachi, Japan). Prior analysis, the cross section of freezing-dried hydrogels was sputtered with gold and scanned at the accelerating voltage of 20 kV. Thermal stability analysis was performed using a simultaneous thermal analyzer (STA449C, NETZSCH, Germany). The transparency of the freshly prepared hydrogels was evaluated by a UV–Vis spectrophotometer (UV-1800, Shimadzu, Japan). Transmittance of the prepared hydrogels with a thickness of 2 mm was recorded over the spectral range 300–800 nm as described by Lv et al. (2019) with some modification. Mechanical property of the prepared hydrogels was analyzed by a rotational rheometer (Haake Mars 60, Germany).

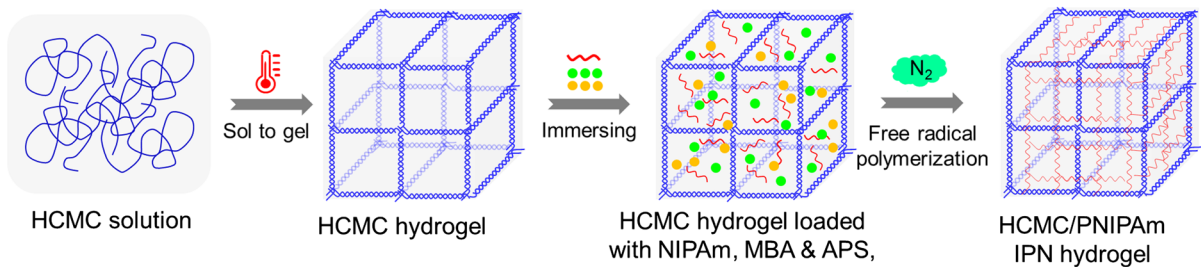### Swelling kinetics of the prepared hydrogels

For swelling kinetics test, the freezing-dried and dimension-uniformed hydrogels (20 ± 2 mg) were immersed into excessive distilled water at room temperature. The swollen hydrogels were carefully taken out at preset time intervals and weighed immediately after removing excess surface water. The swelling degree was calculated according to the following equation:

$$\text{Swelling degree (g/g)} = \frac{m_t - m_d}{m_d} \tag{1}$$

where m_t (g) is the mass of hydrogels at time t (s); m_d (g) is the mass of dried hydrogels.

In order to investigate the dynamic swelling process of the prepared hydrogels, the data from swelling kinetics were analyzed by first-order and second-order kinetics models, respectively. Their linear forms could be expressed as follow:
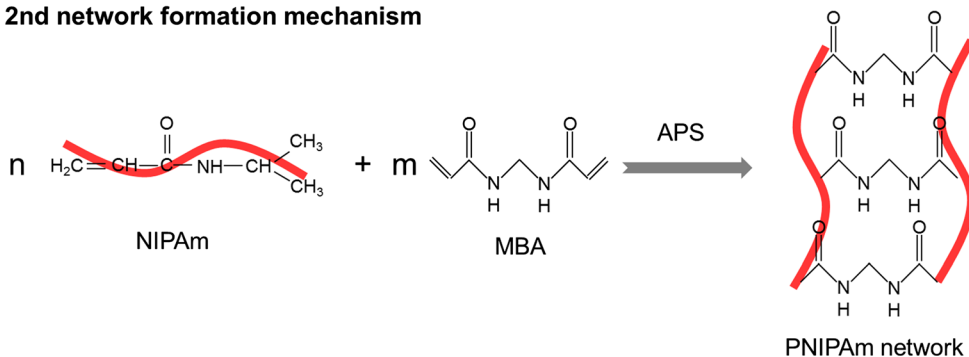
The IPN hydrogel formation process

The 1st network formation mechanism
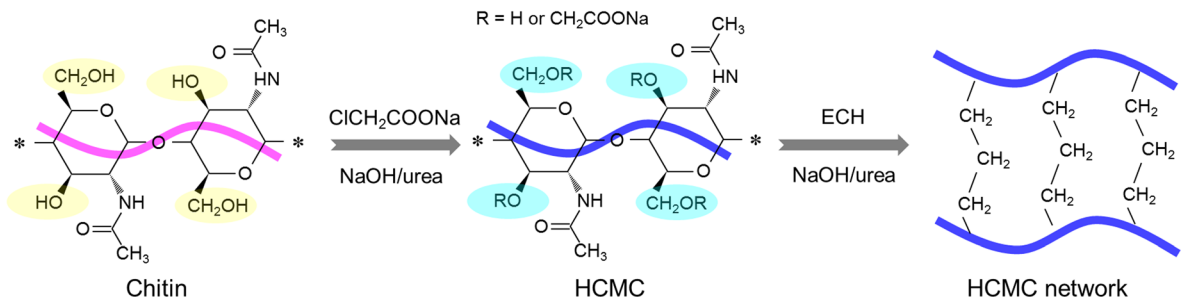
The 2nd network formation mechanism

Scheme 1 Synthetic schematic diagram of CMCH/PNIPAm sequential IPN hydrogels

$$\ln(q_e - q_t) = -\frac{k_1}{2.303}t + \ln q_e \qquad (2)$$

$$\frac{t}{q_t} = \frac{1}{q_e}t + \frac{1}{k_2 q_e^2} \qquad (3)$$

where q_e (g/g) and q_t (g/g) are swelling degree of the prepared hydrogels at equilibrium and at time t (s), respectively; k_1 (g/g s^{-1}) and k_2 (g/g s$^{-0.5}$) are rate constants of the first-order and second-order kinetics models, respectively.

Temperature and pH responsive behavior of the prepared hydrogels

The temperature responsive behavior of the prepared hydrogels was evaluated in distilled water at different temperatures (from 25 to 40 °C). The pH responsive behavior of the prepared hydrogels was evaluated in buffer solutions with desirable pH values (from 1.0 to 11.0) at room temperature. After swelling for 2 h, the swelling degree was calculated according to Eq. (1).

Drug release behavior of the prepared hydrogels

5-Fu was selected as model drug to study the drug release performance of the prepared hydrogels. 5-Fu concentration was determined at 265 nm wavelength using a UV–Vis spectrophotometer (UV-1800, Shimadzu, Japan), based on a previously established calibration curve (Fig. S1). Firstly, the dimension-uniformed hydrogels were immersed into 30 mL 5-Fu solutions (200 mg/L) at room temperature for 24 h to prepare 5-Fu loaded hydrogels. To determine drug loading content, the 5-Fu loaded hydrogels were immersed in 30 mL distilled water with ultrasonic treatment for 30 min, the absorbance of supernate obtained by centrifugation (10000r/min at room temperature for 20 min) was recorded at 265 nm. To evaluate the drug release behavior of the prepared hydrogels, the 5-Fu loaded hydrogels were immersed into 30 mL release medium (at pH 1.2 and 7.4, respectively) under different temperature (at 25 °C and 37 °C, respectively). 1 mL of supernate was taken out at pre-determined time intervals for 5-Fu concentration determination. The removed solution was replaced with an identical volume of fresh releasing solution to keep the volume constant. The results were expressed as cumulative release ratio, which was calculated by the following equation:

$$\text{Cumulative release ratio} \, (\%)$$
$$= \frac{0.03C_n + \sum 0.001C_{n-1}}{m_L} \times 100\% \qquad (4)$$

where C_n and C_{n-1} are the concentration (mg/L) of 5-Fu in the release media at n and n-1 times, respectively; n represents the times of drawing out of the solution; m_L denotes the initial amount (mg) of 5-Fu loaded; 0.03 and 0.001 are the volume (L) of 5-Fu release medium and supernate for 5-Fu concentration measurement, respectively.

To investigate the kinetics of 5-Fu release from the prepared hydrogels, the drug release data were analyzed by Higuchi and Korsmeyer–Peppas models (Korsmeyer et al. 1983):

$$Q_t = K t^{1/2} \qquad (5)$$

$$\ln Q_t = n \ln t + \ln K \qquad (6)$$

where Q_t is fractional 5-Fu release at time t (min), K is a release constant, and n is diffusion exponent characteristic of release mechanism.

Statistical analysis

The data were presented as the means ± standard deviations and evaluated by one-way analysis of variance (ANOVA) using SPSS 21.0 Statistics (SPSS Inc., Chicago, USA). The mean values were compared using independent samples t test. Results with a P value ≤ 0.05 were considered significant.

Results and discussion

Chemical structure analysis

Figure 1a is the representative ATR-FTIR spectra of the prepared hydrogels. All the prepared hydrogels
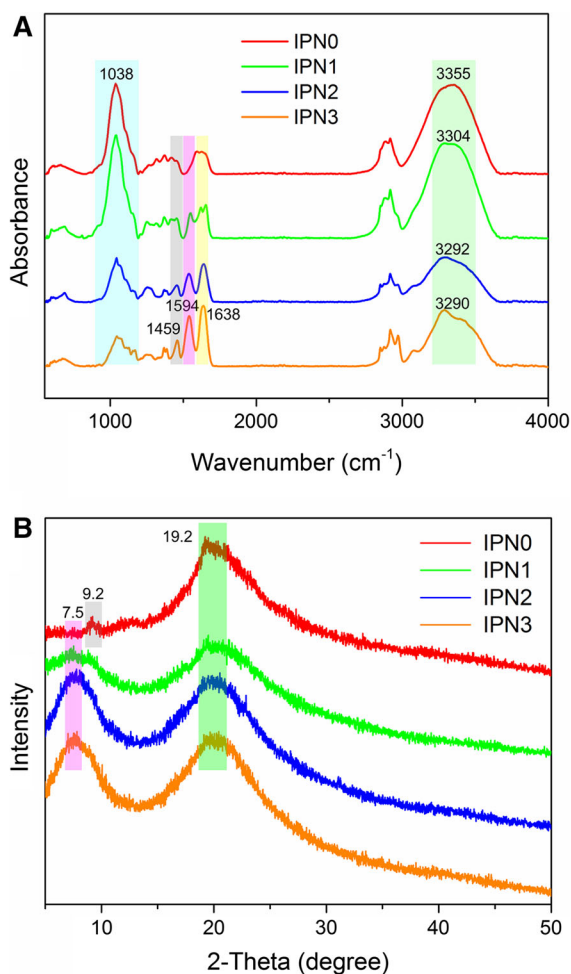

Fig. 1 ATR-FTIR spectra (**a**) and XRD patterns (**b**) of the prepared hydrogels

showed strong absorption peaks at around 3300 and 1038 cm^{-1}, corresponding to O–H and C–OH, respectively (Dai et al. 2019a; Liu et al. 2014). As NIPAm concentration increased, the O–H related peaks exhibited a shift from 3350 cm^{-1} (for IPN0) to 3304, 3292 and 3290 cm^{-1} (for IPN1, IPN2 and IPN3, respectively), and the absorption peaks at 1638 cm^{-1} (amide I vibrations) became stronger, implying the increasing interactions between HCMC and PNIPAm. Compared with IPN0, the other three hydrogels showed two new characteristic peaks at 1459 and 1594 cm^{-1}, corresponding to -CH$_3$ deformation and C=C of NIPAm, respectively (Jaiswal et al. 2010), confirming the presence of PNIPAm network.

Figure 1b is the typical XRD patterns of the prepared hydrogels. For IPN0, two diffraction peaks at 9.2° and 19.2° were observed, corresponding to the characteristic peaks of chitin (Hong et al. 2019), suggesting the crystalline structure was not affected by carboxymethylation and hydrogels preparation process. Compared with IPN0, other hydrogels all showed a new diffraction peak at 7.5°, indicating there were two separated networks in the prepared IPN hydrogels (Jalababu et al. 2018).

Morphological analysis

Figure 2 shows the optical photographs and SEM images of IPN0, IPN1, IPN2 and IPN3. As observed form optical photographs, the IPN0 was almost colorless, while IPN1, IPN2 and IPN3 were white, indicating the synthesis of PNIPAm. Besides, the color of the prepared hydrogels gradually deepened as NIPAm concentration increased. This phenomenon could be attributed to the fact that as NIPAm concentration increased, PNIPAm network was increasingly synthesized inside the HCMC hydrogels, forming more compact hydrogel network.

As depicted in SEM images, these freezing-dried hydrogels all showed well-defined and great 3D porous structures. The polymeric structure with interconnected pores was caused by sublimation of water during freezing-drying, and the pore size was mainly depended on the degree of hydrogel cross-linking (Dragan et al. 2012; Wei et al. 2015). IPN0 showed 3D macroporous structure with pore diameter of around 200 μm, indicating that IPN0 was composed of a flexible polymer chain but with a low chemical crosslink density. However, the pore size gradually

decreased as the increasing of initial NIPAm concentration, implying that the increasing chemical crosslinking occurred due to the increased monomer concentration. In general, the capability of hydrogel to take up water is mainly depended on its average pore size, hydrogels with more compact interior structure have less water holding capacity (Gao et al. 2013). The water content determination results (Fig. S2) also suggested that IPN0 has maximum pore size, followed by IPN1, IPN2 and IPN3, respectively.

Thermal property analysis

The thermal degradation behavior of the prepared hydrogels was studied from 35 to 500 °C under N$_2$ atmosphere. As shown in Fig. 3a, the main weight loss could be divided into 2 stages for IPN0, whereas 3 stages were observed for IPN1, IPN2 and IPN3. All the prepared hydrogels showed a slight weight loss at 35–85 °C, implying the evaporation of moisture; whereas a major weight loss was found at 210–380 °C, mainly due to the decomposition of HCMC chains. In this stage, it could be clearly found that IPN0 showed greater weight loss than IPN1, IPN2 and IPN3. This result might be attributed to the fact that the proportion of HCMC inside IPN hydrogels decreased as the introduction of PNIPAm. In addition, there was another weight loss occurred at 380–430 °C for IPN1, IPN2 and IPN3, which could be attributed to the PNIPAm degradation (Pan et al. 2018). Therefore, the differences in weight loss between IPN0 and other three hydrogels supported the presence of PNIPAm inside HCMC hydrogels.

Figure 3b is the DTG curves of the prepared hydrogels with scanning range from 35 to 500 °C. For IPN0, only one decomposition peak was observed, which was caused by HCMC degradation. For IPN1, IPN2 and IPN3, there were two degradation peaks, corresponding to the degradation of HCMC and PNIPAm, respectively. As observed from Fig. 3c, the first maximum decomposition rate of IPN0, IPN1, IPN2 and IPN3 occurred at 318, 304, 283 and 280 °C, respectively. This result indicated that the introduction of PNIPAm could accelerate the degradation of HCMC. As shown in Fig. 3d, IPN1, IPN2 and IPN3 showed the second maximum degradation peak at 397, 402 and 402 °C, respectively, indicating the presence of PNIPAm.
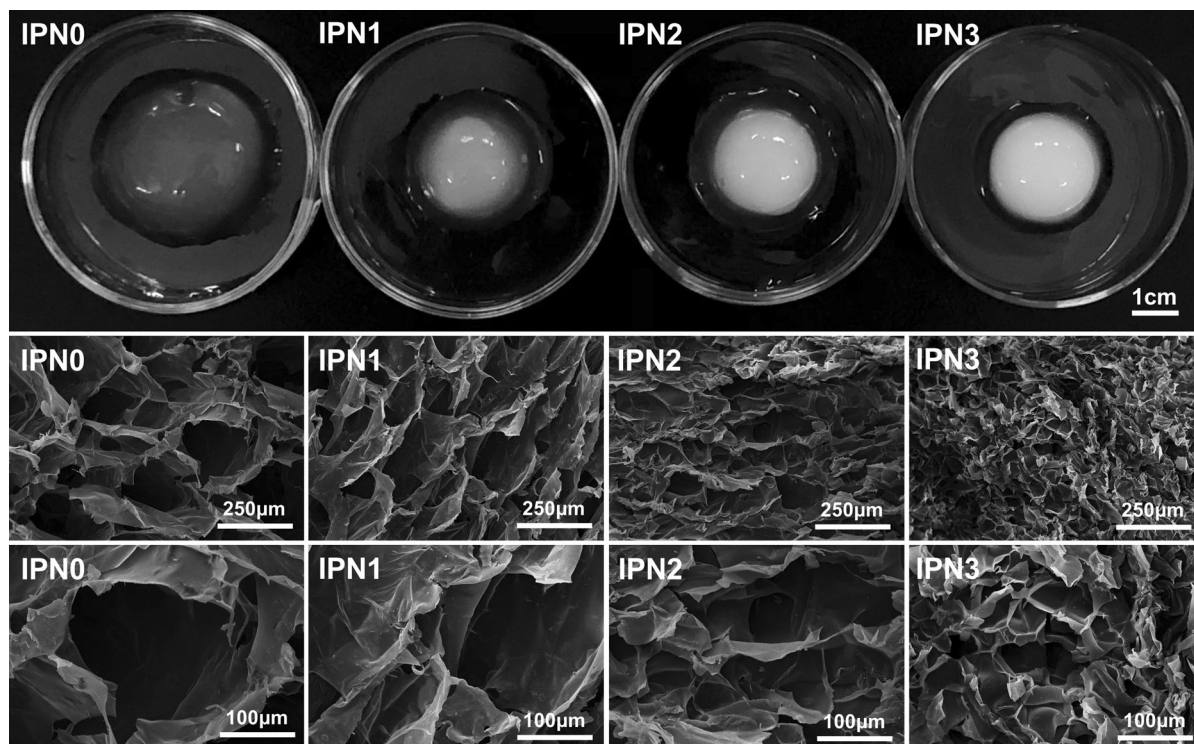
Fig. 2 Optical photographs and SEM images of the prepared hydrogels

Transparency analysis

Figure 4a is the light transmittance (Tr) of the prepared hydrogels within the wavelength range of 300–800 nm. It can be seen that all the prepared hydrogels had transparency (Tr > 0%) within the wavelength range of 320–800 nm, and Tr increased with the increasing wavelength. Under visible light wavelength region (400–800 nm), the prepared hydrogels displayed higher Tr than that at ultraviolet-A (320–400 nm) and ultraviolet-B (300–320 nm) region. In addition, the highest Tr was found for IPN0, followed by IPN1, IPN2 and IPN3 within the tested wavelength range, indicating that the formation of second network could exhaust the transparency of hydrogels. As observed from the inset, all the kapok logo under the hydrogels could be observed under visible light, but it is getting obscure as NIPAm concentration increased, which also supported the light transmittance result described above.

Mechanical property analysis

Angular frequency sweep measurements could reflect the structural integrity and mechanical strength of hydrogels (Yuan et al. 2018). In this study, storage modulus (G′) and loss modulus (G″) as a function of angular frequency were used to evaluate elasticity and viscosity of the prepared hydrogels, respectively. As shown in Fig. 4b, G′ was higher than G″ for all the prepared hydrogels within the tested frequency range, indicating a typical gel-like system and dominant elastic character (Clarke et al. 2017). Besides, G′ and G″ were hardly influenced by the tested angular frequency for all the prepared hydrogels, suggesting a relative stable gel structure (Yang et al. 2018). Gel strength was usually evaluated by complex modulus (G*), expressed as $G^* = \sqrt{G'^2 + G''^2}$, which could be also replaced by G′ when G′ ≫ G″ (Liu et al. 2017a, b). It could be clearly noticed that IPN3 had the maximum G′, followed by IPN2, IPN1 and IPN0, respectively. This result suggested that the formation of IPN structure could increase gel mechanical property.
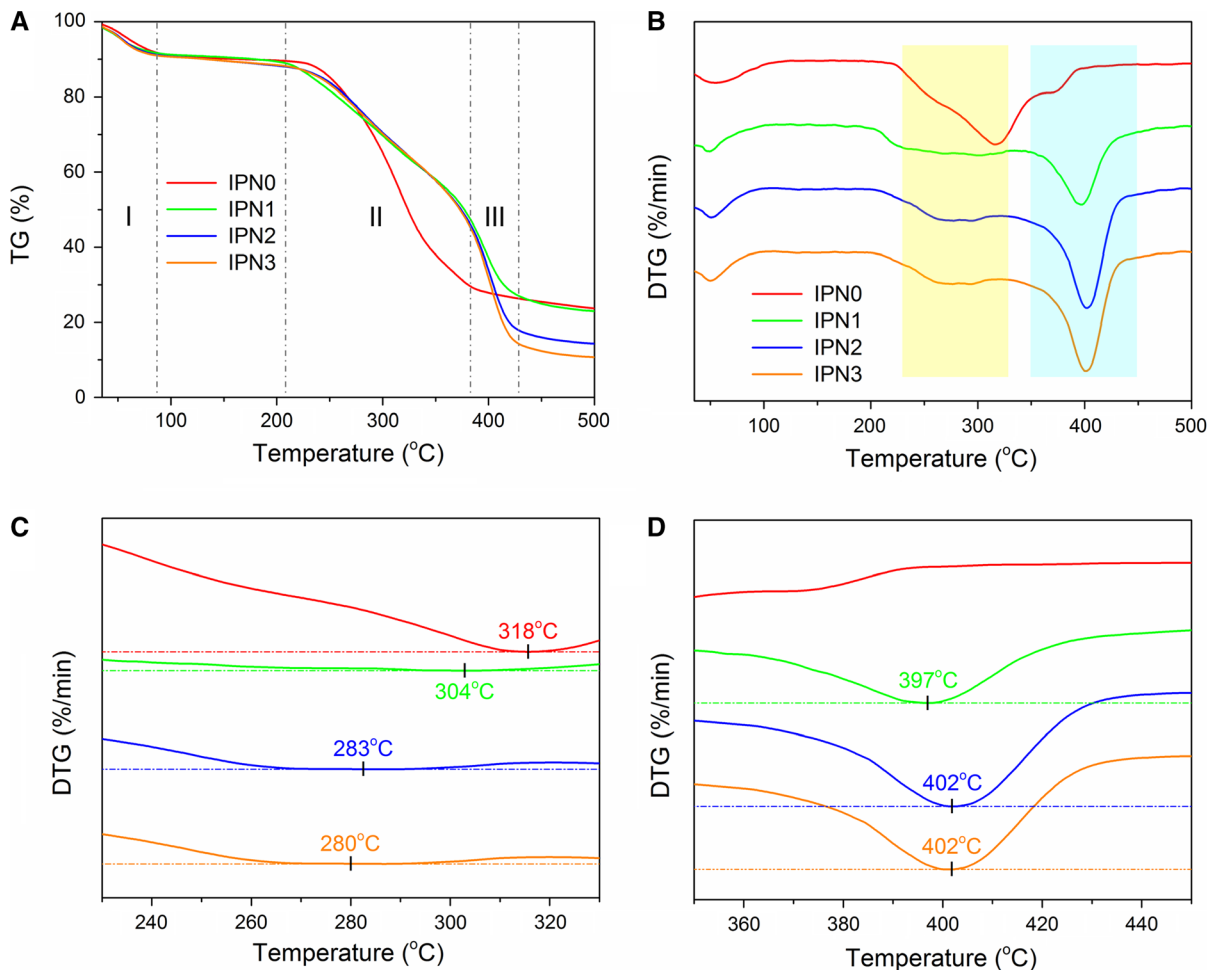
Fig. 3 TG (**a**) and DTG (**b**) curves of the prepared hydrogels from 35 to 500 °C; DTG curves from 230 to 330 °C (**c**); DTG curves from 350 to 450 °C (**d**)

Swelling property analysis

The swelling kinetics curves of the prepared hydrogels in distilled water at room temperature were displayed in Fig. 5a. All the prepared hydrogels exhibited rapid swelling characteristic due to their macroporous structures. Besides, IPN0 showed the maximum swelling degree, followed by IPN1, IPN2 and IPN3, respectively. The reduced swelling degree could be ascribed to that incorporation of PNIPAm into CMCH network resulted in a denser hydrogel network, which was also confirmed by SEM results. The swelling kinetics data were also analyzed by first-order and second-order kinetics models. The fitted plots were shown in Fig. 5b, c, while their corresponding kinetic parameters were listed in Table S1. The linear

correlation coefficients of second-order kinetics model were ranged from 0.9945 to 0.9999, obviously higher than first-order kinetics model (ranged from 0.7873 to 0.9843), suggesting the swelling process was preferred by second-order kinetics model. In addition, the second-order kinetics model also provided nearer calculated values for swelling degree than the first-order kinetics model, further indicating that the swelling process followed second-order kinetics model.

Temperature sensitivity analysis

The thermal responsive behavior of the prepared hydrogels was evaluated by comparison of swelling degree at different temperatures (from 25 to 40 °C).
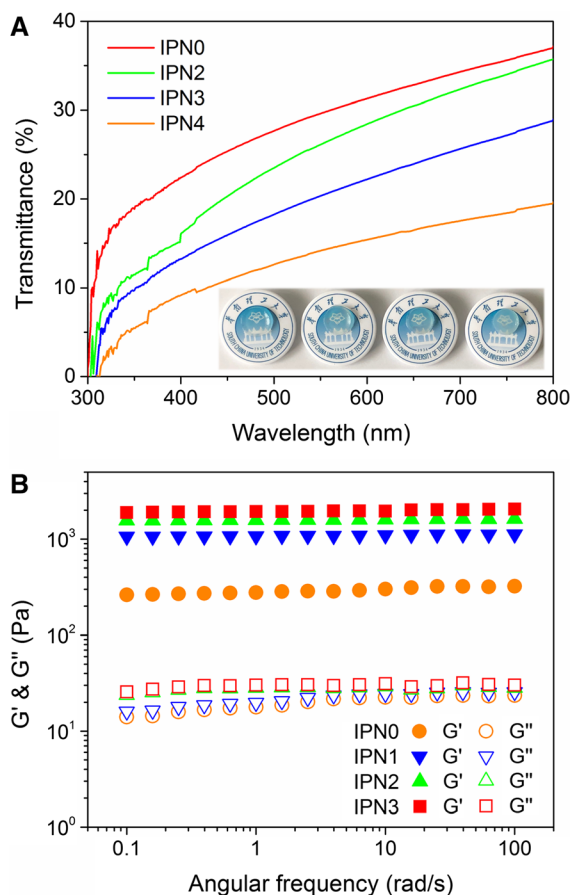
Fig. 4 Light transmittance of the prepared hydrogels (**a**); storage modulus (G') and loss modulus (G'') as a function of angular frequency for all the prepared hydrogels at 25 °C

As shown in Fig. 6a. IPN0 showed nearly constant swelling degree at all tested temperatures; whereas a sharp decrease in swelling degree was observed in the range 34–36 °C for IPN1, IPN2 and IPN3, indicating obvious temperature-dependent swelling characteristic and their LCST is located in this region. This specific behavior is attributed to the fact that PNIPAm is a thermoresponsive polymer, it was expected the PNIPAm based IPN hydrogels could display thermoresponsivity. Generally, temperature sensitivity of PNIPAm hydrogel is attributed to hydrophilic and hydrophobic balance between amide and isopropyl in NIPAm unit (Hirokawa and Tanaka 1984). When temperature is below the LCST, hydrogen bonds would be formed between water molecules and hydrophilic amides, leading to higher swelling degree. Whereas temperature is above the LCST, the formed
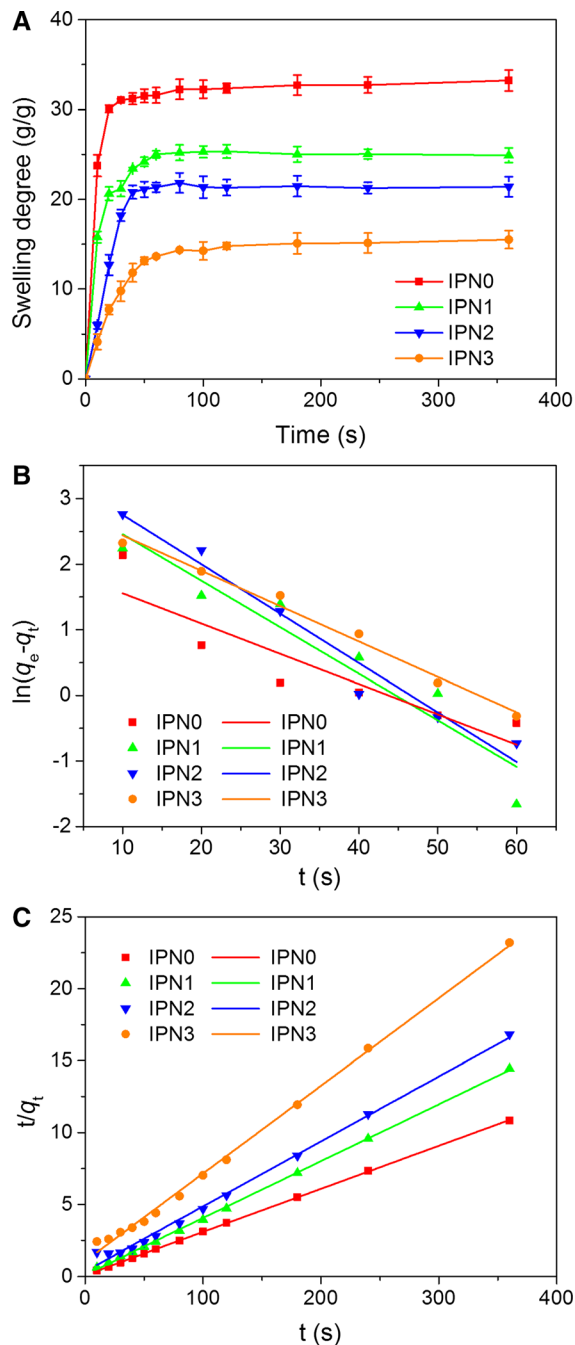

Fig. 5 Swelling kinetics curves (**a**) of the prepared hydrogels and the corresponding plots for first-order kinetics (**b**) and second-order kinetics model (**c**)

hydrogen bonds would be weakened and hydrophobic interactions would play the major roles, resulting in dramatic decrease of equilibrium swelling ratio (Pan et al. 2018; Sun et al. 2019).
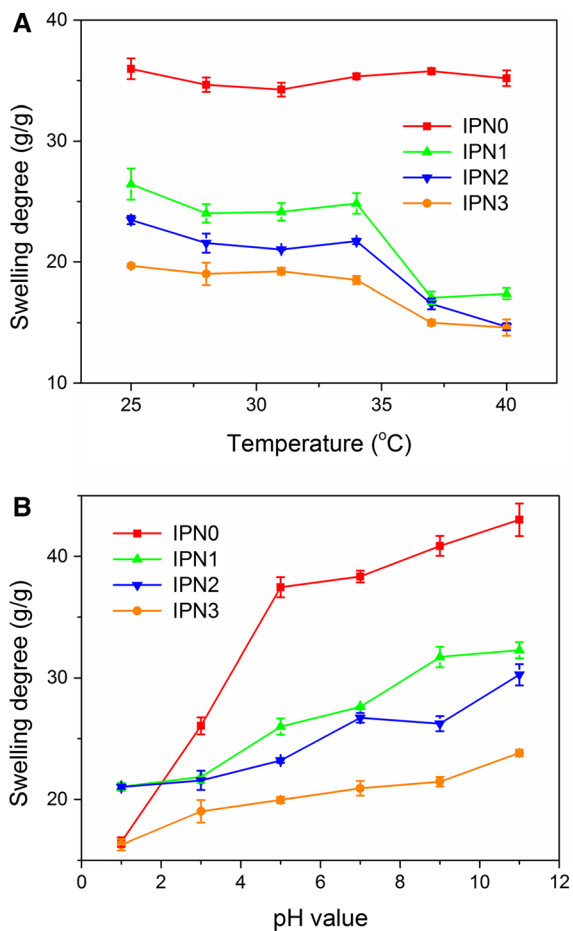
Fig. 6 Swelling capacities of the prepared hydrogels in different temperature (**a**) and pH (**b**)

pH sensitivity analysis

To investigate pH sensitivity of the prepared hydrogels, equilibrium swelling degree of the prepared hydrogels was compared at different pH (from 1.0 to 11.0). As depicted in Fig. 6b, the swelling degree of all the prepared hydrogels increased with pH from 1.0 to 11.0, showing obvious pH-dependent swelling characteristic. This pH sensitivity behavior could be due to the presence of HCMC and explained according to previous reported literatures (Gharekhani et al. 2017; Ma et al. 2007). In acidic environment, carboxyl groups ($–COO^-$) in hydrogels would be transformed into carboxylic acid groups (–COOH), which could strengthen hydrogen-bonding interactions between

–COOH and –OH, resulting in more internal crosslinking and shrinkage of hydrogel network. As pH value increased, –COOH in hydrogel network would be dissociated, and the enhanced electrostatic repulsion among $–COO^-$ contributed to the expansion of the hydrogels network (Sun et al. 2019).

5-Fu release analysis

Effects of formulation parameters

In vitro 5-Fu release behaviors of the prepared hydrogels at different conditions were shown in Fig. 7a, b. Under all the tested conditions, 5-Fu could be gradually released from the prepared hydrogels, which exhibited burst release in the initial 10 min, mainly caused by the release of those 5-Fu located near the hydrogel surface. Beyond the burst period, all the prepared hydrogels showed prolonged 5-Fu release behavior. After 24 h, IPN0 showed the maximum cumulative release ratio, followed by IPN1, IPN2 and IPN3, respectively. Generally, drug release from hydrogels is mainly controlled by interactions between drug and hydrogels, drug solubility and swelling ability of hydrogels (Kim et al. 1992). It could be seen that 5-Fu release profiles were consistent with swelling kinetics curves. This result indicated that the increased PNIPAm network could reduce 5-Fu release. The gradually reduced cumulative release ratio was attributed to the fact that as NIPAm concentration increased, more compact network structure could be formed. Therefore, the drug inside the hydrogels needs to diffuse through more polymer layers to release (Yuan et al. 2018). Based on these results, the 5-Fu release from the hydrogels could be controlled by adjusting the concentration of NIPAm.

Effects of temperatures

Temperature is one of the most universal stimuli to control drug release. In this study, in vitro 5-Fu release experiments were investigated at 25 °C and 37 °C (pH 7.4), respectively. As displayed in Fig. 7a, IPN0 showed similar release profiles at 25 °C and 37 °C, and the corresponding maximum cumulative release ratios were 75.7% and 76.2% ($P > 0.05$),
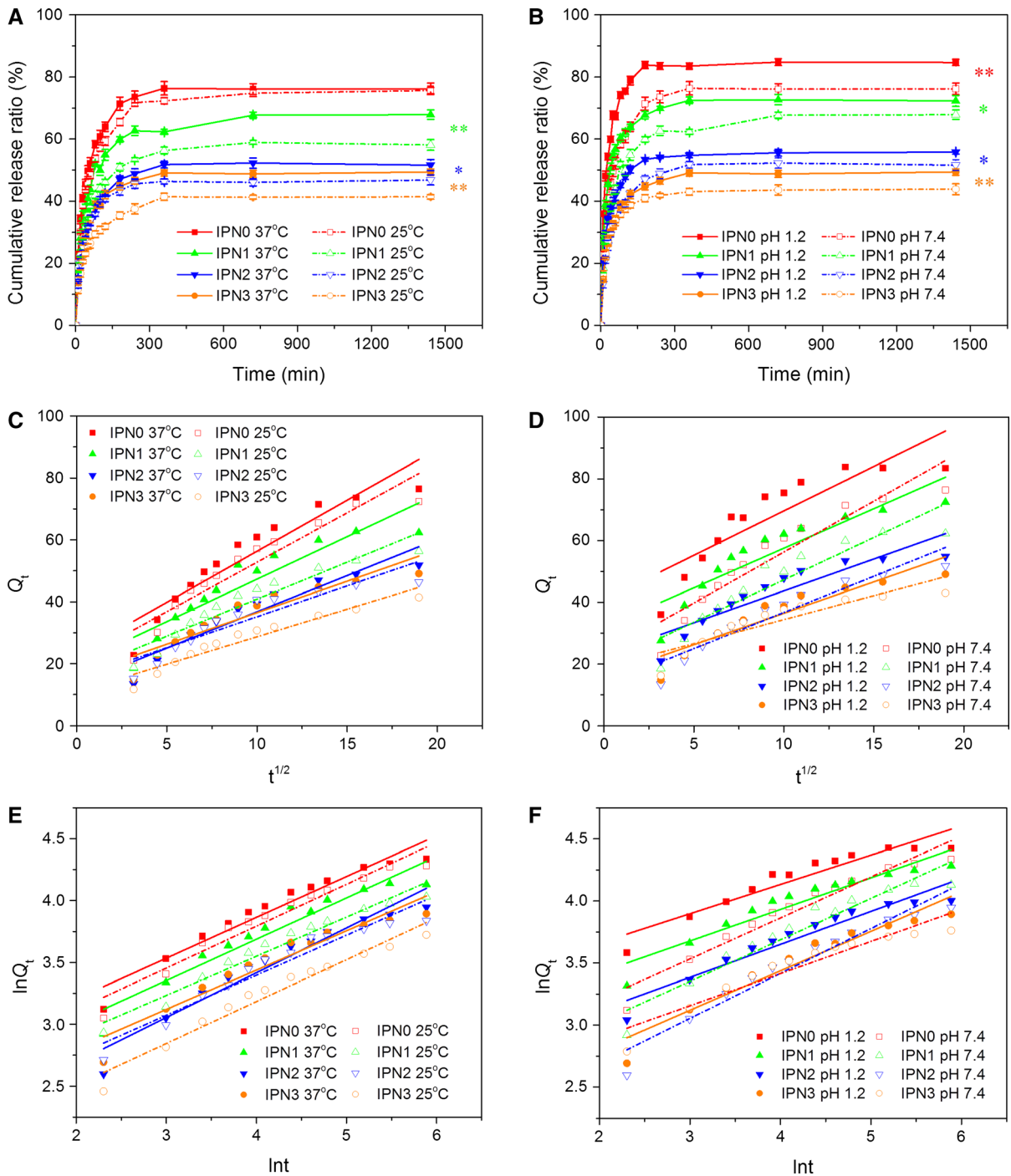
Fig. 7 5-Fu cumulative release curves of the prepared hydrogels at different temperature (**a**) and pH (**b**), and the corresponding kinetics plots of Higuchi (**c**, **d**) and Korsmeyer–Peppas model (**e**, **f**). $*P < 0.05$, $**P < 0.01$ between each group

respectively, indicating IPN0 has no temperature sensitivity. However, the maximum cumulative release ratios of IPN1, IPN2 and IPN3 were 67.9%,

51.6% and 49.4% at 37 °C, respectively, significantly higher than those (58.1%, 46.8% and 41.4% for IPN1, IPN2 and IPN3, respectively) at 25 °C. This result

In vitro 5-Fu controlled release
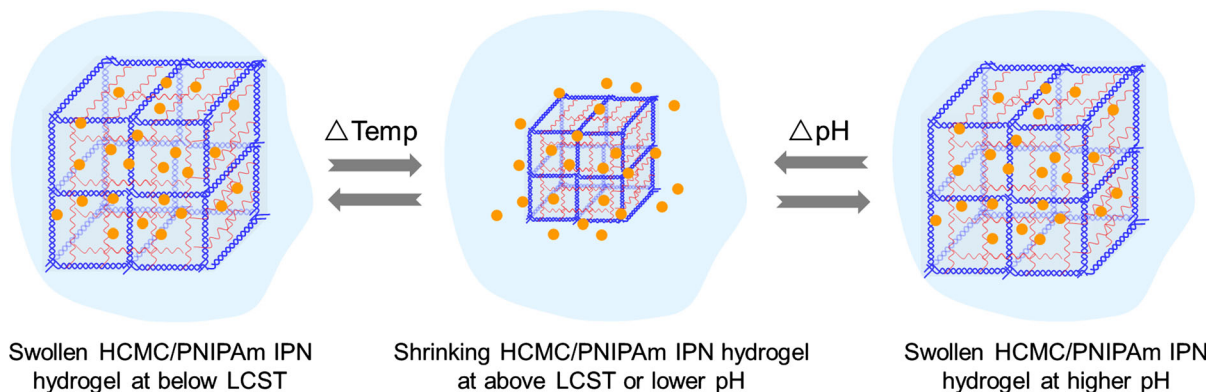
Scheme 2 5-Fu release from HCMC/PNIPAm IPN hydrogels by altering temperature and pH

suggested that IPN1, IPN2 and IPN3 have temperature responsive behavior.

Effects of pH values

pH is another important stimuli for controlling drug release, because pH can be varied at some specific body sites such as stomach and intestine (Karimi et al. 2016). In this study, the 5-Fu release profiles of the prepared hydrogels were investigated at pH1.2 and 7.4, respectively. As shown in Fig. 7b, it could be observed that 5-Fu release weakened as the increase of pH from 1.2 to 7.4 for all tested carriers, 84.6%, 72.3%, 55.8% and 49.4% 5-Fu was released from IPN0, IPN1, IPN2 and IPN3 at pH 1.2, respectively, significantly higher than that at pH 7.4 (76.2%, 67.9%, 51.6% and 43.8% 5-Fu release from IPN0, IPN1, IPN2 and IPN3, respectively) after 24 h, indicating a pH responsive release behavior.

Release kinetics analysis

Higuchi model describes the release of solid drugs randomly dispersed in the solid matrices (Higuchi 1963). While Korsmeyer–Peppas model assumes the release of drugs in porous macromolecule matrix by diffusion through the pores and channels in the network structure (Korsmeyer et al. 1983). In this study, the release kinetics of 5-Fu from the prepared hydrogels were studied by both Higuchi and Korsmeyer–Peppas models. According to release kinetics

data, the fitted curves were shown in Fig. 7c–f and their corresponding kinetic parameters were listed in Table S2. The linear correlation coefficients of Korsmeyer–Peppas model were higher than Higuchi model, suggesting the release process was preferred by Korsmeyer–Peppas model. It has been demonstrated that the value of n could be used to evaluate drug diffusion mechanism: in the case of n < 0.45, it follows Fickian diffusion; In the case of 0.45 < n < 0.89, non-Fickian diffusion is dominant; In the case of n > 0.89, it belongs to case II transport (Dai et al. 2019b). In this study, all the calculated n values were not over 0.45, indicating the 5-Fu release mainly follows Fickian diffusion.

In vitro 5-Fu controlled release analysis

The illustration of 5-Fu controlled release by varying temperature and pH could be summarized in Scheme 2. When temperature is above LCST, the prepared hydrogels would be shrinking. As a result, the porous channels of hydrogels containing PNIPAm would open due to the shrink of the polymer chain, and the entrapped drug molecules would therefore leak out (Lin et al. 2013; Zhang et al. 2013; Pan et al. 2018). On the other hand, a shrinking phenomenon could be also observed when lowering the pH value of release medium due to the protonation of most carboxylate anions. Meanwhile, part of water would be driven out of the hydrogels, resulting in more released drug (Pan et al. 2018).

Conclusion

The HCMC/PNIPAm IPN hydrogels were prepared using fungal chitin as framework followed by in situ free radical polymerization of NIPAm. The mushroom derived chitin could avoid allergy caused by crustacean derived chitin. The initial concentration of NIPAm strongly influenced the internal structure, transparency, mechanical property, swelling kinetics, temperature/pH responses and drug release behavior of the prepared hydrogels. So these characteristics were able to be tunable by varying the initial NIPAm concentrations. More importantly, the presence of HCMC and PNIPAm network afforded the IPN hydrogels capabilities of responding to pH and temperature changes, i.e., swelling and drug release at specific pH and temperature. Therefore, the prepared hydrogels are expected as a promising candidate material in controlled drug delivery systems due to its tunable and smart characteristics.

References

Azarova YA, Pestov AV, Bratskaya SY (2016) Application of chitosan and its derivatives for solid-phase extraction of metal and metalloid ions: a mini-review. Cellulose 23:2273–2289

Bilbao-Sainz C, Chiou BS, Williams T, Wood D, Du WX, Sedej I et al (2017) Vitamin D-fortified chitosan films from mushroom waste. Carbohydr Polym 167:97–104

Chen JP, Cheng TH (2006) Thermo-responsive chitosan-graft-poly (N-isopropylacrylamide) injectable hydrogel for cultivation of chondrocytes and meniscus cells. Macromol Biosci 6:1026–1039

Chien RC, Yen MT, Mau JL (2016) Antimicrobial and antitumor activities of chitosan from shiitake stipes, compared to commercial chitosan from crab shells. Carbohydr Polym 138:259–264

Clarke DE, Pashuck ET, Bertazzo S, Weaver JVM, Stevens MM (2017) Selfhealing, self-assembled beta-sheet peptide-poly(gamma-glutamic acid) hybrid hydrogels. J Am Chem Soc 139:7250–7255

Croisier F, Jérôme C (2013) Chitosan-based biomaterials for tissue engineering. Eur Polym J 49:780–792

Dai H, Ou S, Liu Z, Huang H (2017) Pineapple peel carboxymethyl cellulose/polyvinyl alcohol/mesoporous silica SBA-15 hydrogel composites for papain immobilization. Carbohydr Polym 169:504–514

Dai H, Ou S, Huang Y, Liu Z, Huang H (2018a) Enhanced swelling and multiple-responsive properties of gelatin/sodium alginate hydrogels by the addition of carboxymethyl cellulose isolated from pineapple peel. Cellulose 25:593–606

Dai H, Huang Y, Huang H (2018b) Eco-friendly polyvinyl alcohol/carboxymethyl cellulose hydrogels reinforced with graphene oxide and bentonite for enhanced adsorption of methylene blue. Carbohydr Polym 185:1–11

Dai H, Zhang Y, Ma L, Zhang H, Huang H (2019a) Synthesis and response of pineapple peel carboxymethyl cellulose-g-poly (acrylic acid-co-acrylamide)/graphene oxide hydrogels. Carbohydr Polym 215:366–376

Dai H, Zhang H, Ma L, Zhou HY, Yu Y, Guo T, Zhang Y, Huang H (2019b) Green pH/magnetic sensitive hydrogels based on pineapple peel cellulose and polyvinyl alcohol: synthesis, characterization and naringin prolonged release. Carbohydr Polym 209:51–61

Dragan ES, Lazar MM, Dinu MV (2012) Preparation and characterization of IPN composite hydrogels based on polyacrylamide and chitosan and their interaction with ionic dyes. Carbohydr Polym 88:270–281

Gao XY, Cao Y, Song XF, Zhang Z, Xiao CS, He CL, Chen XS (2013) pH and thermo-responsive poly(N-isopropylacrylamide-co-acrylic acid derivative) copolymers and hydrogels with LCST dependent on pH and alkyl side groups. J Mater Chem B 1:5578–5587

Gharekhani H, Olad A, Mirmohseni A, Bybordi A (2017) Superabsorbent hydrogel made of NaAlg-g-poly(AA-co-AAm) and rice husk ash: synthesis, characterization, and swelling kinetic studies. Carbohydr Polym 168:1–13

Guo Y, Duan B, Cui L, Zhu P (2015) Construction of chitin/graphene oxide hybrid hydrogels. Cellulose 22:2035–2043

Haq MA, Su Y, Wang D (2017) Mechanical properties of PNIPAM based hydrogels: a review. Mater Sci Eng C 70:842–855

Higuchi T (1963) Mechanism of sustained action medication: theoretical analysis of rate of release of solid drugs dispersed in solid matrices. J Pharm Sci 52:1145–1149

Hirokawa Y, Tanaka T (1984) Volume phase transition in a nonionic gel. J Chem Phys 81:6379–6380

Hong S, Yang QR, Yuan Y, Chen L, Song YD, Lian HL (2019) Sustainable co-solvent induced one step extraction of low molecular weight chitin with high purity from raw lobster shell. Carbohydr Polym 205:236–243

Jaiswal MK, Banerjee R, Pradhan P, Bahadur D (2010) Thermal behavior of magnetically modalized poly(n-isopropylacrylamide)-chitosan based nanohydrogel. Colloids Surf B 81:185–194

Jalababu R, Veni SS, Reddy KVNS (2018) Synthesis and characterization of dual responsive sodium alginate-g-acryloyl phenylalanine-poly n-isopropyl acrylamide smart hydrogels for the controlled release of anticancer drug. J Drug Deliv Sci Technol 44:190–204

Karimi M, Ghasemi A, Zangabad PS, Rahighi R, Moosavi Basri SM, Mirshekari H et al (2016) Smart micro/nano particles in stimulus-responsive drug/gene delivery systems. Chem Soc Rev 45:1457–1501

Kim SW, Bae YH, Okano T (1992) Hydrogels: swelling, drug loading, and release. Pharm Res 9:283–290

Korsmeyer RW, Gurny R, Doelker E, Buri P, Peppas NA (1983) Mechanisms of solute release from porous hydrophilic polymers. Int J Pharm 15:25–35

Liao J, Huang H (2019a) Green magnetic hydrogels synthesis, characterization and flavourzyme immobilization based on chitin from *Hericium erinaceus* residue and polyvinyl alcohol. Int J Biol Macromol 138:462–472

Liao J, Huang HH (2019b) Magnetic chitin hydrogels prepared from *Hericium erinaceus* residues with tunable characteristics: a novel biosorbent for Cu^{2+} removal. Carbohydr Polym 220:191–201

Lima BV, Vidal RR, Marques ND, Maia AM, Balaban RD (2012) Temperature-induced thickening of sodium carboxymethylcellulose and poly(n-isopropylacrylamide) physical blends in aqueous solution. Polym Bull 69:1093–1101

Lin X, Ju X, Xie R, Jiang M, Wei J, Chu L (2013) Halloysite nanotube composited thermoresponsive hydrogel system for controlled-release. Chin J Chem Eng 21:991–998

Liu Z, Huang H (2016) Preparation and characterization of cellulose composite hydrogels from tea residue and carbohydrate additives. Carbohydr Polym 147:226–233

Liu J, Liu G, Liu W (2014) Preparation of water-soluble β-cyclodextrin/poly(acrylic acid)/graphene oxide nanocomposites as new adsorbents to remove cationic dyes from aqueous solutions. Chem Eng J 257:299–308

Liu H, Yang Q, Zhang L, Zhuo R, Jiang X (2016) Synthesis of carboxymethyl chitin in aqueous solution and its thermo- and ph-sensitive behaviors. Carbohydr Polym 137:600–607

Liu CM, Guo XJ, Liang RH, Liu W, Chen J (2017a) Alkylated pectin: molecular characterization, conformational change and gel property. Food Hydrocolloids 69:341–349

Liu Z, Li D, Dai H, Huang H (2017b) Preparation and characterization of papain embedded in magnetic cellulose hydrogels prepared from tea residue. J Mol Liq 232:449–456

Lv JH, Sun B, Jin J, Jiang W (2019) Mechanical and slow-released property of poly(acrylamide) hydrogel reinforced by diatomite. Mater Sci Eng C 99:315–321

Ma J, Xu Y, Fan B, Liang B (2007) Preparation and characterization of sodium carboxymethylcellulose/poly(n-isopropylacrylamide)/clay semi-ipn nanocomposite hydrogels. Eur Polym J 43:2221–2228

Munoz G, Valencia C, Valderruten N, Ruiz-Durantez E, Zuluaga F (2015) Extraction of chitosan from *Aspergillus niger* mycelium and synthesis of hydrogels for controlled release of betahistine. React Funct Polym 91–92:1–10

Pan YF, Wang JC, Cai PX, Xiao HN (2018) Dual-responsive IPN hydrogel based on sugarcane bagasse cellulose as drug carrier. Int J Biol Macromol 118:132–140

Roland CM (2013) Interpenetrating Polymer Networks (IPN): structure and mechanical behavior. In: Kobayashi S, Müllen K (eds) Encyclopedia of polymeric nanomaterials. Springer, Berlin

Sun XF, Zeng Q, Wang H, Hao Y (2019) Preparation and swelling behavior of ph/temperature responsive semi-IPN hydrogel based on carboxymethyl xylan and poly(n-isopropyl acrylamide). Cellulose 26:1909–1922

Wei QB, Luo YL, Fu F, Zhang YQ, Ma RX (2013) Synthesis, characterization, and swelling kinetics of pH-responsive and temperature-responsive carboxymethyl chitosan/polyacrylamide hydrogels. J Appl Polym Sci 129:806–814

Wei W, Qi X, Liu Y, Li J, Hu X, Zuo G, Zhang J, Dong W (2015) Synthesis and characterization of a novel pH-thermo dual responsive hydrogel based on salecan and poly (N, N-diethylacrylamide-co-methacrylic acid). Colloids Surf B 136:1182–1192

Wu T, Zivanovic S, Draughon FA, Sams CE (2004) Chitin and chitosan-value-added products from mushroom waste. J Agric Food Chem 52:7905–7910

Yang X, Nisar T, Liang D, Hou Y, Guo Y (2018) Low methoxyl pectin gelation under alkaline conditions and its rheological properties: using NaOH as a pH regulator. Food Hydrocolloids 79:560–571

Yen MT, Mau JL (2007) Selected physical properties of chitin prepared from shiitake stipes. LWT Food Sci Technol 40:558–563

Yuan Y, Wang L, Mu RJ, Gong J, Wang Y, Li Y et al (2018) Effects of konjac glucomannan on the structure, properties, and drug release characteristics of agarose hydrogels. Carbohydr Polym 190:196–203

Zhang X, Yang P, Dai Y, Ma P, Li X, Cheng Z et al (2013) Drug delivery: multifunctional up-converting nanocomposites with smart polymer brushes gated mesopores for cell imaging and thermo/pH dual-responsive drug controlled release. Adv Funct Mater 23:4062

Zhang L, Wang L, Guo B, Ma PX (2014) Cytocompatible injectable carboxymethyl chitosan/N-isopropylacrylamide hydrogels for localized drug delivery. Carbohydr Polym 103:110–118

Zhuo RX, Li W (2003) Preparation and characterization of macroporous poly(-isopropylacrylamide) hydrogels for the controlled release of proteins. J Polym Sci A Polym Chem 41:152–159

Publisher's Note Springer Nature remains neutral with regard to jurisdictional claims in published maps and institutional affiliations.